C., *Plant Cell Rep.*, 1994, **13**, 647–654.
8. Li, L., Qu, R., Kochko, A., Fauquet, C. and Beachy, R. N., *Plant Cell Rep.*, 1993, **12**, 250–255.
9. Murashige, T. and Skoog, F., *Planta*, 1962, **157**, 385–391.
10. Chu, C. C., Wang, C. C., Sun, C. S., Hsu, C., Yin, K. C., Chu, C. Y. and Bi, F. Y., *Sci. Sin.*, 1975, **18**, 659–668.
11. Visarada, K. B. R. S., Sailaja, M., Arti, P., Balachandran, S. M. and Sarma, N. P., *Curr. Sci.*, 1998, **74**, 1004–1008.
12. Bajaj, S. and Rajam, M. V., *Plant Cell Rep.*, 1995, **14**, 717–720.
13. Chowdhry, C. N., Tyagi, A. K., Maheshwari, N. and Maheshwari, S. C., *Plant Cell Tissue Org. Culture*, 1993, **32**, 357–361.
14. Dodds, J. H. and Roberts, L. W., *Experiments in Plant Tissue Culture*, Cambridge University Press, USA, 1995.
15. Hartke, S. and Lorz, H., *Genet. Breed.*, 1989, **43**, 205–214.
16. Raman, R., Chahal, G. S. and Dhaliwal., H. S., *Crop Improv.*, 1994, **21**, 30–36.
17. Peng, J., Kononowicz, H. and Hodges, T. K., *Theor. Appl. Genet.*, 1992, **83**, 855–863.
18. Peng, J., Wen, F., Lister, R. L. and Hodges, T. K., *Plant Mol. Biol.*, 1995, **27**, 91–104.
19. Chu, C. C., in *Plant Biotechnology for Sustainable Development of Agriculture*, China Forestry Publishing House, Beijing, 1996, pp. 66–71.

ACKNOWLEDGEMENT. D.M. thanks University Grants Commission for the research fellowship award.

DEEPIKA MINHAS*
M. V. RAJAM**
ANIL GROVER*

**Department of Plant Molecular Biology and **Department of Genetics, University of Delhi South Campus, Benito Juarez Road, New Delhi 110 021, India*

Trace element distribution and cobalt content in sulphide ores of Kalyadi, Karnataka

Sulphide deposit at Kalyadi (13°03′03″N; 76°24′E) forms an important part of Kalyadi schist belt, which lies between the Holenarsipur and the Nuggihalli schist belts in the western block of Dharwar Craton (Figure 1). Only a limited data is available on trace element distribution and cobalt content in the sulphide ores of Kalyadi[1,2]. Trace element ratios, especially of Co and Ni in pyrite, appear to have the potential to discriminate between magmatic, submarine exhalative and sedimentary origins of metals in ore deposition[1–5]. The present investigation is aimed at reporting additional trace element data of sulphide ores and to understand the distribution of trace elements in sulphide ores, variation of Co/Ni ratio in pyrites, the mode of occurrence of cobalt in sulphide ores at Kalyadi.

The metasedimentaries and meta volcanics exposed in the Kalyadi area form one of the minor greenschist belts of the Karnataka Craton with all the characteristics of greenstone assemblages. The area represents remnants of the oldest volcanic and sedimentary rocks fragmented and engulfed by later Peninsular gneisses. The metasedimentaries include quartzite while meta volcanics are represented by greenschist suite of rocks. These rocks are intruded by ultramafic bodies, younger granites and dolerite dykes. Quartzites and greenschists host sulphide mineralization in Kalyadi. These formations show marked variation in strike varying from 15°N to 60°W with dip ranging from 50 to 85°NE. The area shows three phases of deformation. The earliest deformation (F1) has produced SSE plunging anticlinal fold. Sulphide mineralization is mainly controlled by second phase of folds (F2) with shallow to steep plunge (60–67°) towards N. These folds are accompanied by the development of schistosity in metavolcanics and metasedimentary formations. The area has undergone greenschist facies to lower amphibolite facies metamorphism. The incipient migmatization and their occurrence as enclaves within peninsular gneiss suggest their similarity to Sargur Group.

Mineralization is confined primarily to the volcano-sedimentary sequence with quartzite hosting chalcopyrite + pyrite, extending for about 600 m along 15°N to 40°W with an average width of 25 m. Sulphide mineralization was also observed in the meta-volcanics, which extends for about 300 m along the eastern margin of the quartzite bed with an average width of 15 m. Sulphide mineralization is confined mainly to structurally weak zones such as crest and trough of the folds, foliations, shear-zones, fractures and limbs of the folds, which have been developed during the second phase of deformation. Disseminated sulphides are more conspicuously present in quartzites as pore fillings. The other forms of mineralization like patches, stringers, etc. present in the host rocks have been formed due to remobilization during subsequent deformation events.

The ore assemblage is characterized by a simple mineralogy consisting of pyrite, chalcopyrite, pyrrhotite, magnetite, specularite and pentlandite. Occurrence of native copper from the cores of Kalyadi boreholes has been reported[6]. Vallerite is suspected to be present in the ores[7]. The most common assemblage in the order of abundance is pyrite, chalcopyrite, magnetite and pyrrhotite. Secondary copper minerals such as malachite and azurite encrustations were observed in the surface exposure around the old working.

Chalcopyrite is found to be intimately associated with gangue quartz and other sulphides. Chalcopyrite replaces pyrite along the margins and also forms thin veinlets in earlier sulphides or filling fractures in early formed minerals like pyrite and quartz. The boundary between pyrite and chalcopyrite is often irregular resulting in carries texture of pyrite grains with convex boundary surface projecting into pyrite. Sometimes the replacement of pyrrhotite by chalcopyrite shows a crystallographic control.

Pyrite generally occurs as coarse idiomorphic crystals and belongs to two generations. Pyrite of the first generation occurring in the stratiform ores shows corroded margins and irregular grain boundaries along the contacts with the later generation sulphides. Pyrite also occurs as inclusions in pyrrhotite. Pyrites of the second generation occur as independent euhedral crystals and are very fresh and free from cataclastic effects. Pyrite, with subordinate amounts of chalcopyrite, occurs in the form of thin laminations interlayered with quartz. Fine dissemination of sulphides is also seen in the quartzite.

The ore bearing quartzite has undergone extensive post depositional deformation and metamorphism, which has caused recrystallization of sulphide minerals and remobilization of sulphides along foliation planes and other structurally weaker planes. The deposit is enriched in Fe, Cu and Co with minor concentrations of Cr, Ni, V and Zn. Concentrations of Ni, Cr, V and Co increase while Cu concentration decreases with depth. In general, Cu is concentrated in certain patches. The dolerite dyke cutting the mineralized zone recorded high content of Cr, Ni and V. Zinc content in the deposit is also very low. The higher Cr content in the deposit could have been influenced by the ultramafic intrusives in this area.

The concentration of Co, Ni, V, Cr, Mn and other basemetals in individual sulphide phases (pyrite and chalcopyrite) were determined using SEM–EDX analysis (Jeol–Kevex system) and are shown in Table.1. The interference of other elements during the elemental analysis was minimized by deconvolution of the acquired spectra prior to measurement. The acquired spectra were deconvoluted and those with a chi-squared value of 1 and below were quantified. The measurements in all the analyses have an accuracy of 0.01% with a precision of 5–10%. Pyrites from Kalyadi are enriched in Co, with concentration as high as 3.69% while its concentration in chalcopyrite is less than 0.65%. The concentration of pyrite as well as Co increases with depth indicating the presence of Co in pyrites even at greater depths. On the contrary, Ni concentration is always lower than Co in pyrites at any given level with average Co/Ni ratio varying from 14.14 to 4.1. However, the chalcopyrite registered lower Co/Ni ratio compared to pyrites indicating higher concentration of Ni relative to Co in chalcopyrite.

It has been proposed that hydrothermal pyrites are characterized by > 400 ppm of Co with Co/Ni > 1 and sedimentary pyrites are characterized by < 100 ppm of Co with Co/Ni < 1 (ref. 8). Further, cobalt concentration in pyrites associated with volcanogenic Cu rich sulphide deposits is relatively higher[9] than the pyrites associated with volcanogenic Pb–Zn sulphide deposits (Ni and Co < 10 ppm; Co/Ni < 1)[10]. Also, it has been suggested that pyrites associated with volcano-sedimentary massive sulphide deposits are characterized by Co/Ni ratios > 5 and commonly > 10 (refs 3, 4, 11). In Kalyadi, pyrite has higher Co/Ni ratio by virtue of the higher content of cobalt. The Co/Ni ratios are > 1 in all the analysed grains. The high content of cobalt in pyrites has been attributed to the presence of linneite ($(CoNi)_3S_4$) as the minor phase[1]. The maximum cobalt content recorded during the present study and also reported earlier[2] in Kalyadi pyrites is 3.69% (Table 1) and 8.15%, respectively and the Co content in linneite is 57.9% (ref. 12), thus this data precludes the presence of linneite as a minor phase in Kalyadi ores. Further, in order to confirm whether or not separate cobalt-bearing phase is present in pyrites of Kalyadi, several grains of pyrites rich in cobalt (Co = 3.69%) have been hand-picked for SEM–EDX and X-ray diffraction analyses. The results shows that Co is occurring within the pyrite lattice, replacing Fe and not as a separate phase.

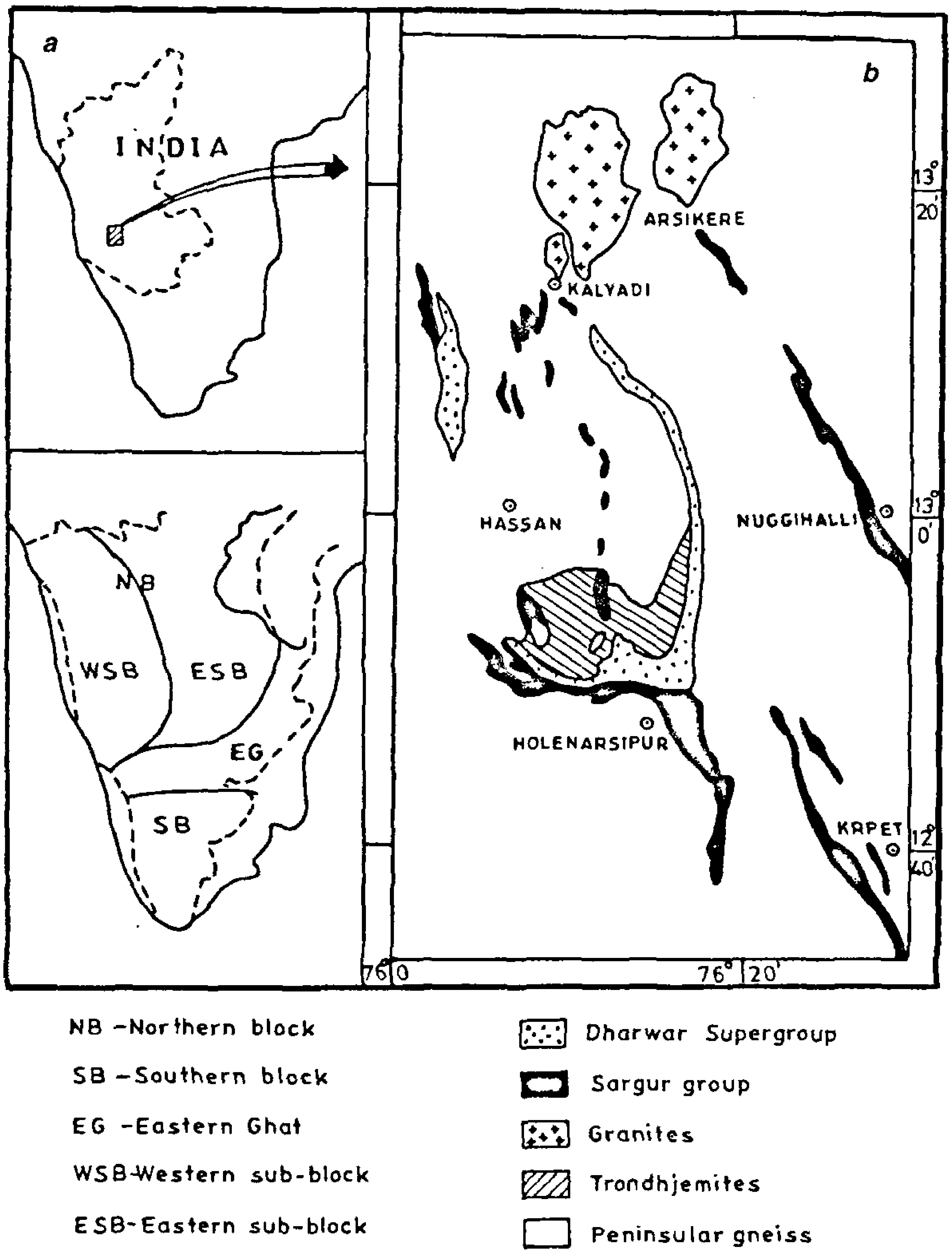

Figure 1. Geological map showing position of Kalyadi schist belt between Nuggihalli and Holenarsipur schist belts.

Table 1. SEM–EDX analysis of sulphides from Kalyadi (in wt%)

	No. of spots analysed	S	V	Cr	Mn	Fe	Co	Ni	Cu	Co/Ni
Pyrite 1	4	50.85–51.64	0.08–0.10	0.12–0.17	0–0.23	46.25–46.96	0.89–1.29	0.15–0.25	0.42–0.50	3.56–8.60
Pyrite 2	6	50.81–51.72	0.11–0.20	0–0.19	0.13–0.30	46.14–47.19	0.64–1.17	0.19–0.28	0.31–0.51	2.30–5.60
Pyrite 3	5	50.17–52.08	0.10–0.19	0.11–0.18	0.16–0.26	45.75–47.28	0.71–1.22	0.16–0.33	0.27–0.50	2.73–6.44
Pyrite 4	6	51.40–52.13	0.08–0.16	0.09–0.16	0.13–0.24	45.90–46.74	0.50–1.06	0.21–0.28	0.35–1.42	2.38–5.05
Pyrite 5	6	51.31–52.34	0.07–0.16	0.12–0.18	0.15–0.27	44.02–47.04	0.51–2.47	0.23–0.32	0.34–0.84	1.89–9.88
Pyrite 6	3	51.45–53.58	0.10–0.12	0.06–0.15	0.10–0.28	44.88–46.79	0.64–0.84	0.11–0.29	0.47–0.61	2.90–6.27
Pyrite inclusion	1	51.39	0.07	0.1	0.17	46.47	0.82	0.18	0.33	4.556
Chalcopyrite 1	4	32.06–33.22	0.10–0.15	0.15–0.20	0–0.26	30.30–30.80	0.33–0.52	0.25–0.37	35.16–36.22	0.95–2.08
Chalcopyrite 3	3	45.16–45.78	0.08–0.10	0.06–0.11	0.14–0.17	40.19–40.53	0.41–0.51	0.21–0.33	12.84–13.35	1.52–2.43
Chalcopyrite 4	1	35.59	0.05	0.1	0.12	29.4	0.32	0.19	34.24	1.684
Chalcopyrite 5	1	33.94	0.09	0.1	0.17	30.15	0.37	0.35	34.82	1.057
Chalcopyrite 6	4	32.19–32.96	0.10–0.13	0.11–0.19	0.16–0.34	30.06–30.62	0.31–0.53	0.33–0.36	35.7–36.29	0.91–1.55
Pyrite 1	7	50.61–52.80	0.10–0.20	0.18–0.28	0.38–0.48	44.84–47.16	0.54–0.93	0.07–0.18	0.21–0.53	4.11–7.71
Pyrite 2	5	51.54–53.45	0.11–0.22	0.17–0.33	0.43–0.58	44.88–46.71	0.41–0.64	0.09–0.18	0.18–0.29	3.56–5.89
Pyrite 3	7	50.71–53.24	0.14–0.31	0.24–0.36	0.44–0.70	44.88–47.40	0.46–0.67	0.07–0.11	0.12–0.30	4.70–7.00
Chalcopyrite 1	3	33.92–35.95	0.10–0.22	0.12–0.23	0.27–0.38	29.21–30.14	0.32–0.49	0.29–0.42	33.74–34.38	1.10–1.35
Chalcopyrite 2	3	33.39–33.81	0.16–0.25	0.19–0.29	0.33–0.38	29.97–30.34	0.48–0.61	0.37–0.47	34.32–34.51	1.19–1.29
Chalcopyrite 3	2	33.09–33.68	0.56–0.66	0.45–0.55	0.62–0.74	29.96–30.15	0.54–0.58	0.40–0.45	33.75–33.81	1.20–1.45
Co pyrite 1	6	51.94–52.54	0.07–0.13	0.09–0.12	0.14–0.19	43.19–45.55	0.96–3.69	0.14–0.24	0.28–0.43	6.85–20.50
Co pyrite 2	6	52.09–52.78	0.07–0.19	0.08–0.16	0.13–0.23	43.52–45.07	1.65–3.30	0.09–0.23	0.30–0.49	9.70–19.33
Co pyrite 3	7	51.82–52.84	0.05–0.12	0.11–0.15	0.16–0.26	44.78–45.83	1.45–2.00	0.12–0.24	0.19–0.33	6.92–16.67
Chalcopyrite 1	3	32.63–35.14	0.04–0.10	0.05–0.12	0.06–0.26	29.41–30.65	0.24–0.44	0.13–0.25	34.94–35.56	1.76–2.00
Chalcopyrite 2	1	28.96	0.2	0.23	0.29	33.73	0.75	0.5	35.35	1.5
Chalcopyrite 3	3	33.18–34.49	0.09–0.13	0.12–0.15	0.09–0.16	30.05–30.57	0.26–0.56	0.20–0.34	34.67–35.41	1.14–2.33
Chalcopyrite 4	2	32.92–33.46	0.08–0.13	0.09–0.12	0.18–0.23	29.91–30.45	0.43–0.48	0.31	34.90–35.97	1.39–1.55

From the Table 1, it is apparent that Kalyadi pyrites from stratiform sulphide ores have Co/Ni ratio higher (2–10) than the pyrites of sedimentary origin (Co/Ni = 0.8)[3,11] and are similar to the Big Cadia Copper deposit in Australia and other Canadian and Chinese Archean Copper deposits of probable exhalative origin[13,14]. Further, the Ni concentration in Kalyadi pyrites is lower relative to pyrites associated with submarine exhalative sulphide deposits. Thus Co and Ni values in Kalyadi pyrites indicate their derivation from a volcanogenic source. The remobilized hydrothermal vein type ores show lower Co content as well as a low Co/Ni ratio than the stratiform type of ores[15]. Thus the primary stratiform ores are enriched in cobalt.

1. Subba Rao, D. V. and Naqvi, S. M.,, *Miner. Deposita*, 1997, **32**, 230–242.
2. Devaraju, T. C. and Alapieti, T. T., *J. Geol. Soc. India*, 1997, **49**, 597–598.
3. Bralia, A., Sabatini, G. and Troja, F., *Miner. Deposita*, 1979, **14**, 353–374.
4. Mookherjee, A. and Philip, R., *Miner. Deposita*, 1979, **14**, 33–55.
5. Campbell, F. A. and Ethier, F. G., *Can. Mineral.*, 1984, **22**, 503–506.
6. Narasimhan, M. and Viswanatha, M. N., Geol. Surv. India, Interim Report, 1970, p. 46.
7. Narahari, E. D., *Rec. Geol. Sur. India*, 1980, **113**, 46–50.
8. Carstens, C. W., *Nor. Geol. Tidsskr.*, 1941, **21**, 231–221.
9. Price, B. J., M Sc thesis, University of British Columbia, 1972.
10. Loftus-Hills, G. and Solomon, M., *Miner. Deposita*, 1967, **2**, 55–65.
11. Green, S. R., Solomon, M. and Walshe, G. L., *Eco. Geol.*, 1981, **76**, 304–338.
12. Kullerud, G. and Yund, R. A., *J. Petrol.*, 1962, **3**, 126–175.
13. Bajwah, Z. U., Seccombe, P. K. and Offler, R., *Miner. Deposita*, 1987, **22**, 292–300.
14. Song, X., *Miner. Deposita*, 1984, **19**, 95–104.
15. Biju Mathew and Chandrasekharam, D., *Indian Mineral.*, 1998, **32**, 69.

BIJU MATHEW
D. CHANDRASEKHARAM

Department of Earth Sciences,
Indian Institute of Technology,
Powai,
Mumbai 400 076, India

Component community structure of larval trematodes in the snail *Cerithium scabridum* from southern Kuwait Bay

Our knowledge about the ecology of parasites has been substantially enriched by studies on larval trematode communities in snail intermediate hosts. Esch and Fernandez[1] reviewed various factors contributing to structuring of trematode communities and concluded that behaviour of the definitive hosts and population dynamics of the intermediate hosts are among the major external factors while interspecific antagonistic interactions among larval forms is the major internal factor.

Members of the gastropod family Cerithidae, also known as creepers or ceriths, are common inhabitants of sandy and muddy intertidal zones of tropical and subtropical coasts. Larval forms representing all major groups of trematodes have been reported in ceriths from different geographical regions; the Great Barrier Reef[2,3], the Caribbean[4,5], the Gulf of Mexico[6], Japan and adjacent territories[7], and the Mediterranean[8]. In Kuwait Bay, Abdul-Salam *et al.*[9] reported 9 cercarial types in the cerith *Clypeomorus bifasciata* (Sowerby 1855). The present study presents information on the component community of larval trematodes parasitizing a population of *Cerithium scabridum* Philippi, 1848 from a site south of Kuwait Bay.

C. scabridum occurs in large aggregates on sand overlaying limestone platform along the Amiri beach in Kuwait city, southern Kuwait Bay. The beach is completely exposed twice a day. During a low tide, the vast intertidal zone is a major habitat for large populations of indigenous and migratory aquatic birds. Samples of *C. scabridum* were collected at monthly intervals from October 1997 to March 1998. Snails were studied by crushing the shell and examining the tissues for larval stages under a dissecting microscope. The larvae were examined live, unstained or vitally stained with 5.0% neutral red. Details of the life cycles of all of the recovered trematodes are not known and they can only be identified to family level according to their diagnostic features, as described by Cable[4] and Schell[10].

A total of 2072 snails ranging in shell height from 5.0 to 17.0 mm were examined, and 83 (4.0%) were infected with 12 species of trematodes representing 8 families. Prevalence of the trematodes and their probable life cycles are shown in Table 1. Highest prevalence was recorded for microphallid II (1.45%) followed by the philophthalmid (1.30%), and the overall prevalence increased with snail shell height (Figure 1). Multiple larval infection was not encountered in any of the examined snails.

In Kuwait Bay, *C. scabridum* is involved in the life cycle of at least 12 species of trematodes, 9 are known to occur as adults in aquatic birds. The trematode fauna in the snail was dominated by microphallid II. A preliminary survey of intertidal crabs and the gull *Larus argentatus* from the study area revealed common occurrence of infections with microphallid metacercariae and adults, respectively. The overall prevalence of infections increased exponentially with shell size (age), a common phenomenon in marine[11,12] as well as fresh water[13]

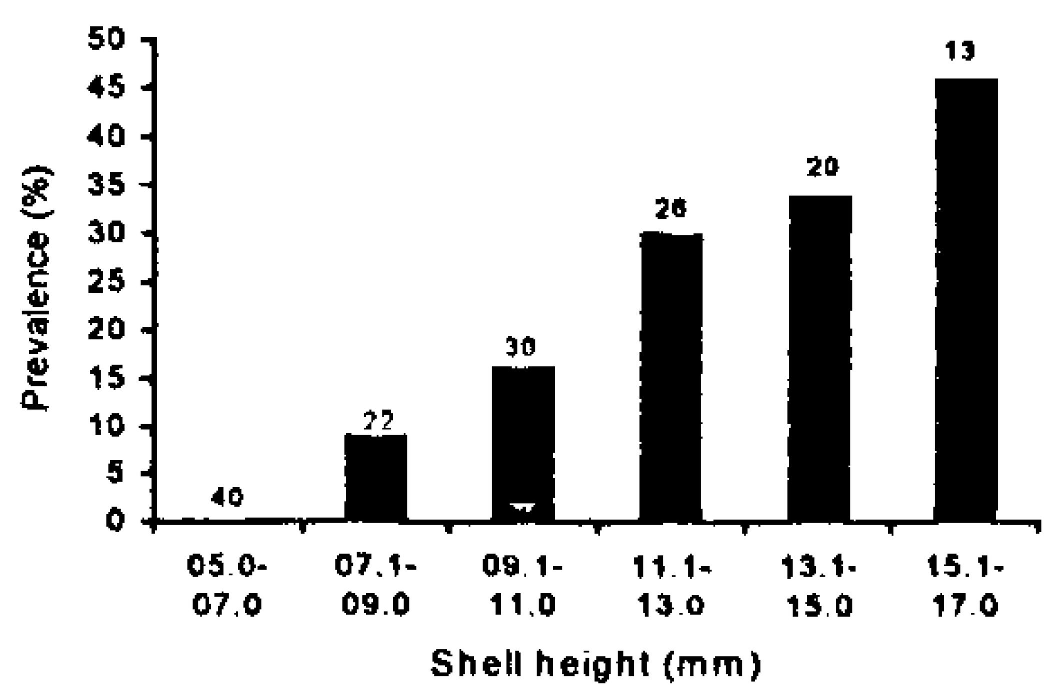

Figure 1. Prevalence of larval trematode infections relative to shell height of the snail *Cerithium scabridum* from Kuwait Bay. The number of snails examined is indicated at the top of each bar.